Available online at www.sciencedirect.com
SCIENCE DIRECT®
International Journal of Heat and Mass Transfer 47 (2004) 5211–5218
International Journal of HEAT and MASS TRANSFER
www.elsevier.com/locate/ijhmt

Buoyant convection in a cubical enclosure under time-periodic magnetizing force

Ki Hyun Kim, Jae Min Hyun *

Department of Mechanical Engineering, Korea Advanced Institute of Science and Technology, 373-1 Kusong-dong, Yusong-gu, Daejon 305-701, South Korea

Received 5 May 2004; received in revised form 25 June 2004

Abstract

A numerical investigation is made of buoyant convection of a paramagnetic fluid in a cubical enclosure under constant gravity g_0. Conventional buoyant convection arises by maintaining different temperatures at two opposite vertical sidewalls. The other walls are thermally insulated. To this basic layout, an electric wire is placed below the bottom horizontal wall to produce a magnetic field. The magnetizing force is induced, which modifies the convective flow and heat transfer characteristics. Comprehensive numerical solutions have been acquired to the governing equations. Of interest are the cases when the strength of the magnetizing force is time-periodic. The computed results reveal the presence of resonance, which is characterized by maximal amplification of the fluctuations of heat transport in the interior. The flow is shown to resonate to the basic mode of internal gravity oscillations. The study points to the feasibility of using the time-periodic magnetizing force as an effective regulator of the convective fluid system.
© 2004 Elsevier Ltd. All rights reserved.

1. Introduction

In a very strong magnetic field, an ordinary (non-ferrous) fluid, such as air, is subjected to the magnetizing force. The strength of this force is proportional to the magnetic susceptibility of the fluid. Understanding the nature of this force and possible industrial utilization has received renewed interest in recent years, spurred by the advent of superconducting magnet.

The flow patterns and associated transport characteristics of a fluid under the magnetizing force have been documented for several specific exemplary systems [1–5]. In particular, the alterations induced in fluid convection and combustion were investigated mostly by numerical and experimental endeavors. Tagawa et al. [5] performed a numerical study of Rayleigh–Benard convection of water in the bore space of a superconducting magnet. It was demonstrated that the fluid flow can be controlled by an effective use of the magnetizing force. Here, the flow induced by the magnetizing force should be distinguished from the more familiar situation of MHD (magneto-hydrodynamics) flow. In the latter, the main dynamic component is the Lorentz force, and the working fluid should be electrically-conducting.

A literature survey reveals that the majority of previous work dealt with the steady-state convective flow induced by the magnetizing force [1–5]. The objective of the present study is to illustrate the feasibility of controlling the convective fluid system by using the magnetizing force, which is externally imposed in a time-periodic

* Corresponding author. Tel.: +82 42 869 3012; fax: +82 42 869 3210.
E-mail address: jmhyun@kaist.ac.kr (J.M. Hyun).

0017-9310/$ - see front matter © 2004 Elsevier Ltd. All rights reserved.
doi:10.1016/j.ijheatmasstransfer.2004.06.015

Nomenclature

$\vec{b}, \vec{B}$	dimensional and non-dimensional magnetic induction, $\vec{B} = \vec{b}/b_a$
b_a	$\mu_m i/L$
d	diameter of the electric coil
e	distance between the electric coil and the bottom of cube
f	frequency of the magnetizing force fluctuation
$\vec{f}_m$	magnetizing force, Eq. (2)
g_0	gravity acceleration
i	electric current in the coil
L	length of the cube
p, P	dimensional and non-dimensional pressure, $P = \frac{(p+\rho g_0 y)L^2}{\rho\kappa^2 Ra\,Pr}$
Pr	Prandtl number, ν/κ
$\vec{r}, \vec{R}$	dimensional and non-dimensional position vector, $\vec{R} = \vec{r}/L$
Ra	Rayleigh number based on gravity acceleration, $g_0\alpha\Delta T L^3/\nu\kappa$
Ra_b	Rayleigh number of the basic state, Eq. (10)
$\vec{s}, \vec{S}$	dimensional and non-dimensional periphery line of the coil, $\vec{S} = \vec{s}/L$
$d\vec{S}$	non-dimensional tangential vector element of the coil
T	temperature
T_0	average temperature, $(T_h + T_c)/2$
ΔT	temperature difference, $(T_h - T_c)$
u, v, w	velocity in the x-, y- and z-direction
U, V, W	non-dimensional velocity in the X-, Y- and Z-direction, $(U,V,W) = (uv,w)(Ra\,Pr)^{-1/2}L/\kappa$
$\vec{V}$	non-dimensional velocity vector
x, y, z	Cartesian coordinates
X, Y, Z	non-dimensional Cartesian coordinates, $(X,Y,Z) = (x,y,z)/L$

Greek symbols

α	volumetric expansion coefficient
χ	mass magnetic susceptibility
γ	relative magnetic effect, $\chi b_a^2/\mu_m g_0 L$
κ	thermal diffusivity of fluid
μ_m	magnetic permeability
ν	kinematic viscosity of fluid
θ	non-dimensional temperature, $(T-T_0)/\Delta T$
ρ	density
τ	non-dimensional time, $\tau = t(Ra\,Pr)^{1/2}\frac{\kappa}{L^2}$
ω	non-dimensional frequency of the magnetizing force, $\omega = f/((Ra\,Pr)^{1/2}\frac{\kappa}{L^2})$

Subscripts

c	cold wall
h	hot wall

manner. For this purpose, convection of air in the much-studied differentially-heated cubical enclosure, placed in a steady uniform gravitational field, $g_0\hat{k}$, is considered. The temperatures at the two vertical sidewalls are respectively T_h and T_c, ΔT $(\equiv T_h - T_c) > 0$. To this conventional differentially-heated buoyancy driven cube, an externally-imposed magnetic field, varying in a time-periodic manner, is applied. In realistic situations, the time-periodic magnetic field can be created with relative ease by controlling the electric current to the coils of a superconducting magnet.

In the present flow layout, the magnetizing force is treated as a body force, similar to the buoyant force. For purely buoyant convective systems under gravity, the preceding studies [6–12] established that resonance occurs when the frequency of external forcing matches the characteristic natural frequencies of the fluid system. Resonance is characterized by maximal amplification of the amplitudes of fluctuation of flow and heat transfer [6]. Parallel studies [10] disclosed that, for a differentially-heated cavity under gravity, the basic mode of the system was shown to be the frequency of internal gravity oscillation.

Numerical computations are made in the present study of the governing equations, which were formulated for the convective system in a cube modified by the magnetic effect. It is shown that, by choosing a correct frequency of the time-periodic externally-imposed magnetic field, considerable augmentation of the fluctuating amplitudes of flow and heat transfer can be realized. This reinforces the belief that a strong external magnetic field can be utilized as an effective regulator of the flow and transport phenomena of the buoyant convective fluid system.

2. Formulation

The flow configuration is sketched in Fig. 1(a). A differentially-heated cubical enclosure of length L, is located, with uniform gravity acting downward (Z-axis) $\vec{g}_0$.

The temperatures at the vertical sidewalls at $X = 0$ and $X = L$ are T_c and T_h, respectively, with $\Delta T(\equiv T_h - T_c) > 0$. The other walls are thermally insulated. A horizontal electric coil of diameter d is positioned at $Z = -e$, below the bottom horizontal wall ($Z = 0$).

The magnetic induction $\vec{b}$ caused by the electric coil, carrying the current i, is described by Biot–Savart's law, i.e.,

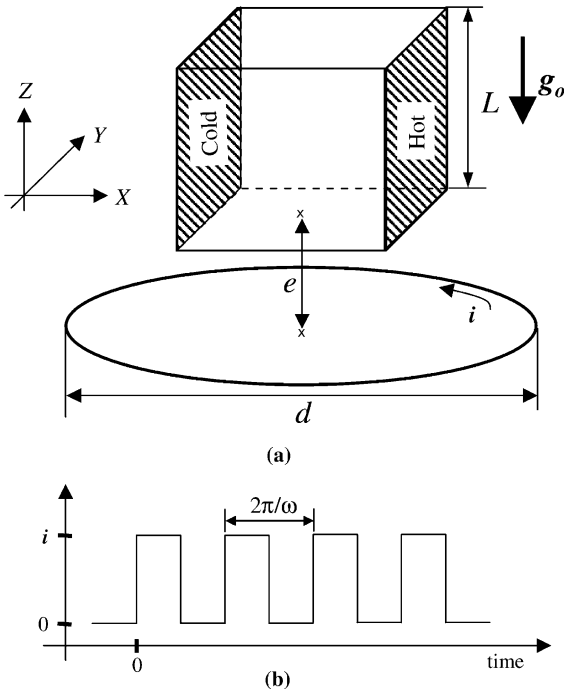

Fig. 1. (a) Flow layout. (b) Time-periodic electric current.

$$\vec{b} = -\frac{\mu_m i}{4\pi}\oint \frac{\vec{r}\times d\vec{s}}{r^3}. \tag{1}$$

In the above, μ_m denotes the magnetic permeability of fluid, and $\vec{r}$ the position vector to the element of the coil $d\vec{s}$.

The magnetizing force $\vec{f}_m$, under the magnetic field $\vec{b}$, can be represented as [1–5]

$$\vec{f}_m = \frac{\rho\chi}{2\mu_m}\vec{\nabla}b^2. \tag{2}$$

In the above, ρ stands for the fluid density, and a key property of the fluid is χ, the magnetic susceptibility. For a paramagnetic substance, the magnetic susceptibility χ is inversely proportional to the absolute temperature, i.e., $\chi = C/T$, where C is a constant [1]. Therefore, if there are temperature inequalities in the system, gradients of χ are induced, which gives rise to unbalanced magnetizing forces. The role of the magnetizing force is similar to that of the usual gravitational buoyancy force, and these aspects have been amply discussed [3–5].

The basic equations governing the buoyancy-driven convective fluid flow, modified by the magnetizing force, have been formulated [3–5]. The Boussinesq-fluid approximation ($\rho = \rho_r[1-\alpha(T- T_r)]$, α being the coefficient of volumetric expansion and subscript r the reference state) is invoked for the density–temperature relationship.

The equations for a paramagnetic fluid, in non-dimensional form, are

$$\nabla\cdot\vec{V} = 0, \tag{3}$$

$$\frac{D\vec{V}}{D\tau} = -\nabla P + \left(\frac{Pr}{Ra}\right)^{1/2}\nabla^2\vec{V} + \theta\left[-\gamma F(\tau)\nabla B^2 + \begin{pmatrix}0\\0\\1\end{pmatrix}\right], \tag{4}$$

$$\frac{D\theta}{D\tau} = \left(\frac{1}{PrRa}\right)^{1/2}\nabla^2\theta. \tag{5}$$

$$\vec{B} = -\frac{1}{4\pi}\oint\frac{\vec{R}\times d\vec{S}}{R^3}. \tag{6}$$

In the above, non-dimensionalization was implemented as follows:

$$\tau = t(RaPr)^{1/2}\frac{\kappa}{L^2},\quad (U,V,W) = (u,v,w)(RaPr)^{-1/2}\frac{L}{\kappa},$$
$$(X,Y,Z) = (x,y,z)/L,$$

$$\theta = \frac{(T-T_0)}{\Delta T},\quad P = \frac{(p+\rho g_0 y)L^2}{\rho\kappa^2 RaPr},\quad B = b/b_a,$$
$$b_a = \frac{\mu_m i}{L},\quad \vec{R} = \frac{\vec{r}}{L},\quad \vec{S} = \frac{\vec{s}}{L},$$

$$Ra = \frac{g_0\alpha\Delta TL^3}{\nu\kappa},\quad Pr = \frac{\nu}{\kappa},\quad \gamma = \frac{\chi b_a^2}{\mu_m g_0 L}.$$

It is noted that the gravity-induced buoyancy effect is measured by Ra, and the influence of magnetizing force, relative to the gravity effect, is represented in γ [3–5] Also, it is remarked that time is made dimensionless by using the reciprocal of the Brunt–Väsällä frequency, $N \equiv (RaPr)^{1/2}\kappa/L^2$. In a stratified fluid in buoyant convection, N indicates the degree of stratification.

In the present problem setting, the effect of time-periodic magnetic field is modeled by switching the current in the electric coil periodically between the ''on'' and ''off'' modes with frequency f. This is incorporated in $F(\tau)$ in the right-hand-side of Eq. (4), in which $F(\tau)$ describes a square wave form with non-dimensional period $2\pi/\omega$, $\omega \equiv f/N$. Accordingly, as shown in Fig. 1(b),

$$F(\tau) = \left\{\begin{array}{ll}1 & \text{for } 2\pi n/\omega < \tau < \pi/\omega + 2\pi n/\omega\\ 0 & \text{for } \pi/\omega + 2\pi n/\omega < \tau < (n+1)2\pi/\omega\end{array}\right\},$$

where n is the number of cycle.

It should be mentioned that, in practical applications using a super-conducting magnet, it is a difficult task to control the magnetic strength in a strictly square wave form. The square wave form envisioned in the present study represents an idealized situation to explore the

fundamental characteristics of buoyant convection under the influence of time-periodic magnetic field.

The boundary conditions are stated as:

$$\begin{aligned} &U = V = W = 0 \text{ on the wall} \\ &\theta = -0.5 \quad \text{at } X = 0, \\ &\theta = 0.5 \quad \text{at } X = 1, \\ &\partial\theta/\partial Y = 0 \quad \text{at } Y = 0, 1, \\ &\partial\theta/\partial Z = 0 \quad \text{at } Z = 0, 1. \end{aligned} \tag{7}$$

The numerical solution to the above system of equations is acquired by adopting the well-established SIMPLER algorithm [13]. Typically, a $(50 \times 50 \times 50)$ mesh network was deployed, and grid stretching was implemented. The QUICK scheme [14] was utilized for the non-linear convective terms. The time step used was $\Delta\tau = 2\pi/(1024\omega)$. The present numerical methodologies and computational details have been widely tested and validated. The grid- and time step-sensitivity and convergence tests were conducted, and the outcome was successful. As to the computational procedures, no claims of innovativeness or novelty are made here; the calculations were carried out in a routine manner.

In the course of analyzing the computed flow data, the heat transport across the vertical cross-section is of interest. This is represented by the Nusselt number Nu at $X = a$, which is defined as

$$Nu_{X=a} = \int_0^1 \int_0^1 \left[U\theta(Ra\,Pr)^{1/2} - \frac{\partial\theta}{\partial X} \right]_{X=a} \mathrm{d}Y\,\mathrm{d}Z$$

As an example of code validation, the steady-state Nusselt number of the present computations is compared against the results of previous investigations [3]. For this exemplary coil arrangement, two coils are placed (one above the top wall, and the other below the bottom wall), which produced a cusp-shaped magnetic field. The computed Nu values of the present study are consistent with the published results, as shown in Table 1.

Table 1
Cross-comparisons of the results for a cusp-shaped magnetic field ($Ra = 10^5$, $Pr = 0.71$, $d/L = 1.5625$, $e/L = 0.28125$)

	No gravity	Gravity + magnetic	
	$\gamma Ra = 10^5$	$\gamma = 1.0$	$\gamma = 10.0$
Tagawa et al. [3]	2.870	4.301	6.786
Present results	2.83	4.280	6.851

3. Results and discussions

Numerical solutions were secured for the parameter values in line with the prior computations for steady-state flows [3–5]: $Ra = 10^7$, $Pr = 0.7$, $e/L = 0.4$, $d/L = 2.0$, $\gamma = 1.0$, 3.0, 5.0 and 10.0, and $\omega = 0.1$–1.4. In the

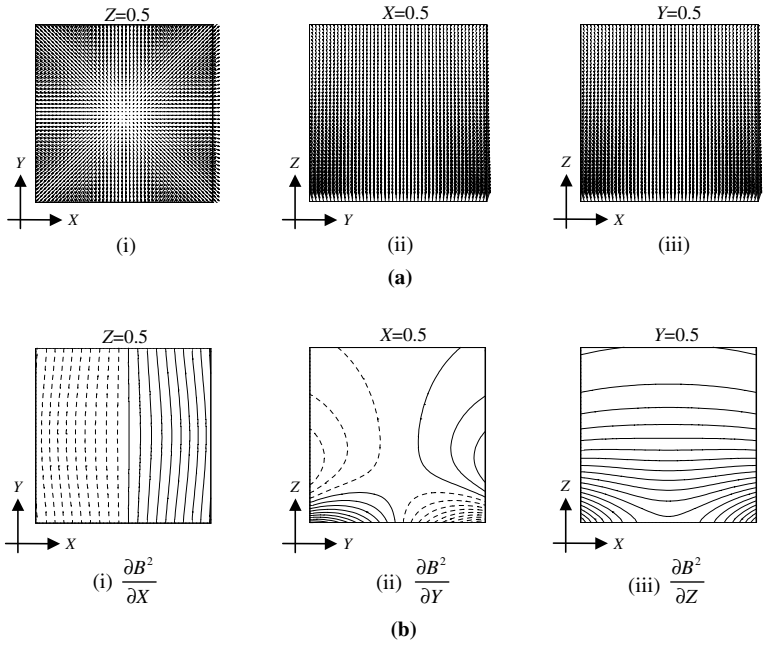

Fig. 2. (a) Computed magnetic induction vectors: (i) $Z = 0.5$ plane; (ii) $X = 0.5$ plane; (iii) $Y = 0.5$ plane. (b) Computed results of the gradients of square of magnetic induction. Solid lines-negative values, and dashed lines-positive values: (i) $Z = 0.5$ plane, $\Delta(\partial B^2/\partial X) = 0.0026$, Max $|\frac{\partial B^2}{\partial X}| = 0.082$; (ii) $X = 0.5$ plane, $\Delta(\partial B^2/\partial Y) = 0.0086$, Max $|\frac{\partial B^2}{\partial Y}| = 0.082$; (iii) $Y = 0.5$ plane, $\Delta(\partial B^2/\partial Z) = 0.027$, Max $|\frac{\partial B^2}{\partial Z}| = 0.081$.

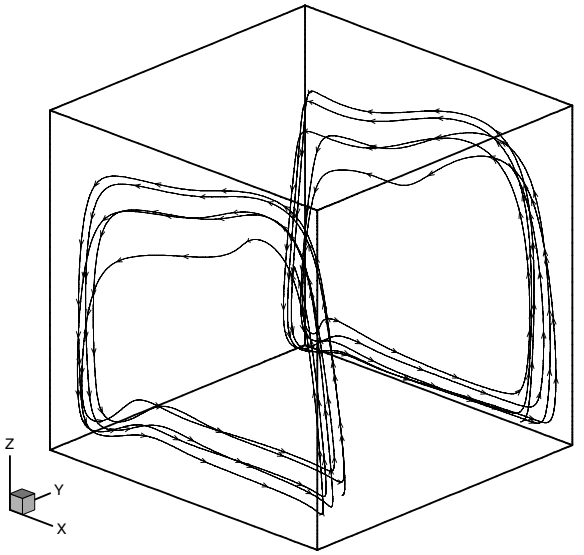

Fig. 3. Computed results of streak lines ($\gamma Ra = 10^7$, $Pr = 0.7$).

real system (air, $L = 0.1$ m), $\gamma = 10.0$ corresponds to $b_a = 6.16T$, and the components (b_x, b_y, b_z) of $\vec{b}_{\text{cubic center}}$ are $(0.009, 0.009, 1.232)T$.

In processing the data, it is useful to monitor the amplitude of fluctuation $A(\phi)$ of a time-periodic variable ϕ over a cycle:

$$A(\phi) = \frac{\text{Max}[\phi(\tau)] - \text{Min}[\phi(\tau)]}{2}, \quad \tau_0 \leqslant \tau \leqslant \tau_0 + 2\pi/\omega.$$

3.1. Cases of steady magnetic field

The magnetic field, which is induced by the steady current in the electric field, is depicted in Fig. 2. Obviously, in order to compute the magnetizing force, it is important to examine the gradient of the magnetic induction squared in each direction, which is illustrated in Fig. 2(b). It is discernible that the Z-direction gradient ($\partial B^2/\partial Z$) is order-of-magnitude larger than the gradients in the X- or Y-directions. This justifies the treatment of the magnetizing force in the right-hand-side of Eq. (4), which was pointed out in [5]. Simply, in the present formulation, the flow system is subjected to the dominant vertically(Z)-downward magnetizing force, which is similar to the conventional vertically-downward gravity.

In an effort to single out the impact of the magnetizing force, computations were conducted for the case of a steady magnetic field in the zero-gravity environment. In this case, as stipulated in [3–5], the parameter γRa is a finite quantity. Fig. 3 exemplifies the computed streaklines for $Pr = 0.7$ and $\gamma Ra = 10^7$. Flows are concentrated to the boundary regions close to the YZ-plane vertical walls of the cubic enclosure. When viewed in the direction of the Y-axis, distinct counter-clockwise circulating flows are seen. The velocity vector plots in the XZ-plane (at $Y = 0.5$) and the temperature field are displayed in Fig. 4. As is apparent in Figs. 3 and 4, the magnetizing force, with zero gravity, produces a boundary layer-type flow adjacent to the YZ-vertical walls, and a nearly stagnant interior region is observed. Also, the temperature field in the interior is well stratified in the vertical direction. Clearly, these plots are akin to those of the conventional buoyant convection in a differentially-heated cavity in the constant-gravity environment [15–18].

3.2. Cases of periodic magnetic field under constant gravity

As ascertained previously, the thrust of the present task is to inquire as to the possibility of flow control, by using a time-periodic magnetic field, in a conventional buoyant convective system under $\vec{g} = \vec{g}_0$.

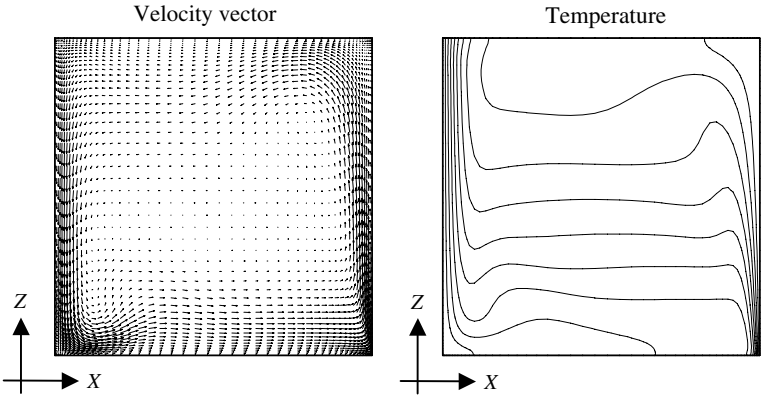

Fig. 4. Temperature and velocity vector fields under steady magnetic and zero-gravity field. At $Y = 0.5$ plane ($\gamma Ra = 10^7$, $Pr = 0.7$ and $\Delta\theta = 0.1$).

As illustrated in Fig. 1(b), by the switching operation of the electric current in the coil, the strength of magnetic field fluctuates between 0 and γ, with period $2\pi/\omega$. The case of non-oscillating magnetic field strength of $\gamma/2$ will be referred to as the basic steady-state configuration. In the numerical computations, the solution to the above-referenced steady basic state was obtained first. This solution was used as the initial condition in computing the cases of time-periodic magnetic field. In most cases, the solution settles to a quasi-steady periodic state after several cycles.

Fig. 5 shows the temporal behavior of $Nu(\tau)$ at the vertical midplane X=0.5. The fluctuation of $Nu(\tau)$ at a particular moderate value of ω ($\omega \cong 0.72$ for $\gamma = 3.0$, $\omega \cong 0.85$ for $\gamma = 10.0$) is much larger than those at smaller or larger frequencies. Compilation of the numerical results, as demonstrated in Fig. 6, points to the observation that the $Nu(\tau)$-fluctuation is maximized at a particular value of ω. This is suggestive of the existence of resonance [6–12]. The $A(Nu)$–ω plots of Fig. 6 indicate that $A(Nu)$ does not change much at low frequencies. In a narrow band surrounding $\omega \cong \omega_r$, $A(Nu)$ is amplified substantially. As ω is increased beyond ω_r, $A(Nu)$ decreases rapidly. It is recalled that the $A(Nu)$–ω behavior shown here is qualitatively similar to that of a purely thermally-driven buoyancy convection [6–12].

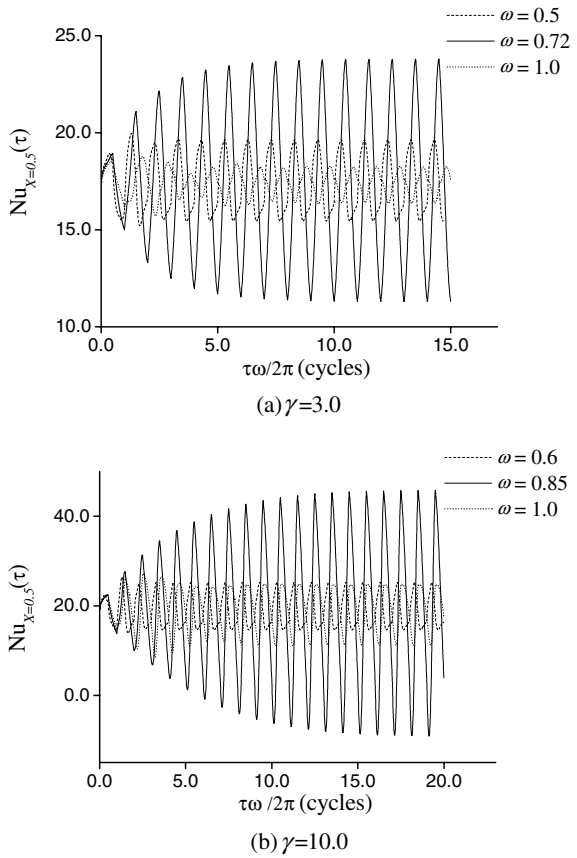

Fig. 5. Time-periodic behavior of the Nusselt number at the vertical mid-plane $X = 0.5$ ($Ra = 10^7$, $Pr = 0.7$).

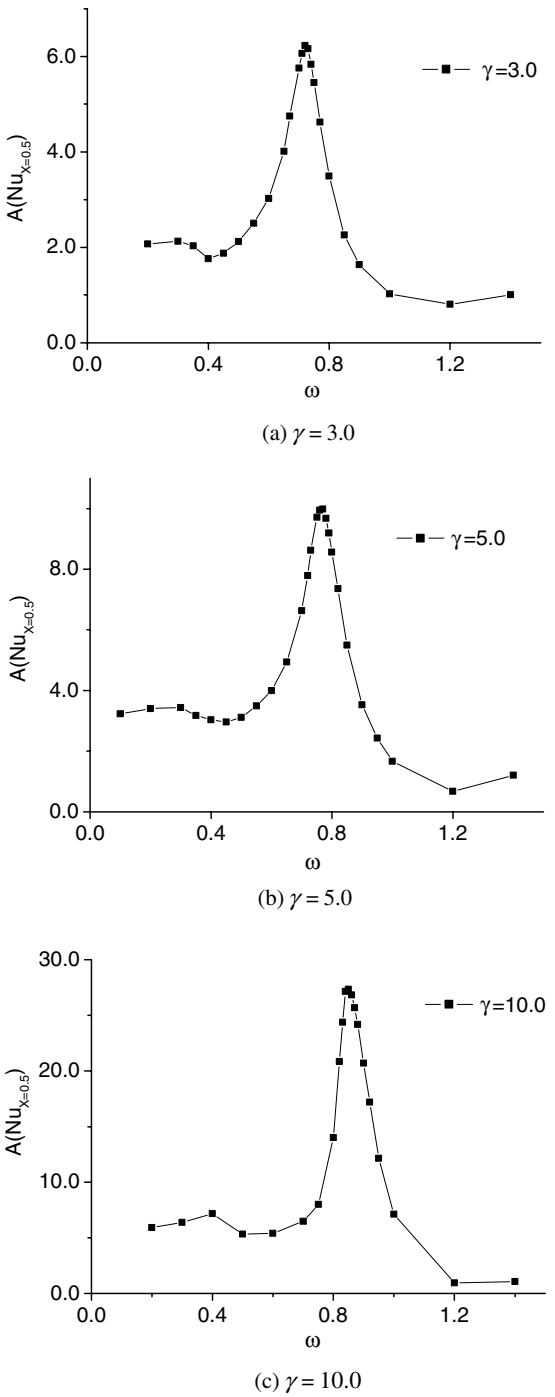

Fig. 6. $A(Nu_{X=0.5})$ variation with ω ($Ra = 10^7$, $Pr = 0.7$).

The preceding studies on time-periodic thermal convection [9–12] argued that resonance is anticipated when the basic mode of natural oscillation of the fluid system is excited. The characteristic natural frequency in a convection with the background gravity was identified to be the internal gravity oscillation mode [9–12]. The fundamental mode of these oscillations was estimated by Paolucci and Chenoweth [19] as

$$f_i = \frac{S(Ra_b Pr)^{1/2}\kappa/L^2}{\sqrt{2}}, \tag{8}$$

which can be non-dimensionalized in the present formulation as

$$\omega_i = \left(\frac{Ra_b}{Ra}\right)^{1/2} \frac{S}{\sqrt{2}}. \tag{9}$$

In the above, $S(\cong \sqrt{\partial\theta/\partial Z})$ represents the overall stratification in the vertical direction in the interior, and Ra_b denotes the Rayleigh number of the non-fluctuating basic state.

In accord with the developments of [9], S is calculated by using a linear fitting to the averaged vertical temperature distribution at the vertical mid-plane $X = 0.5$. As to the estimation of Ra_b, it is noted that, by adding the steady non-fluctuating vertical magnetizing force, the system can be considered to be subject to an enhanced effective steady background gravity. This is made up of the standard terrestrial gravity g_0, plus the vertically-directed magnetizing force produced by the steady current $i/2$ in the coil, as shown in Fig. 1(b), i.e.,

$$Ra_b = \left(1 + \frac{1}{2}\gamma \int_0^1 \int_0^1 \int_0^1 \frac{\partial B^2}{\partial Z}\, dX\, dY\, dZ\right) Ra. \tag{10}$$

Comparisons are shown in Table 2 between the estimated resonance frequencies (based on (9) and (10)) and the results from the numerical computations. Clearly, agreement between the two sets is satisfactory for all the computations covered in the present efforts.

Time-histories of thermal and velocity fields under resonance over a cycle are depicted in Fig. 7. The periodic tilting of isotherms in the interior is notable, which invigorates the flow and convective transport process. These observations were discussed in the earlier studies [9], and these are consistent with the assertion that the global flow resonates with the internal gravity wave oscillation.

Table 2
Comparisons of the estimated resonance frequencies (Eq. (9)), ω_i, and the numerical results, ω_r ($Ra = 10^7$, $Pr = 0.7$)

γ	Ra_b	ω_i, Eq. (9)	ω_r, numerical results
3.0	1.23×10^7	0.74	0.72
5.0	1.39×10^7	0.78	0.77
10.0	1.78×10^7	0.88	0.85

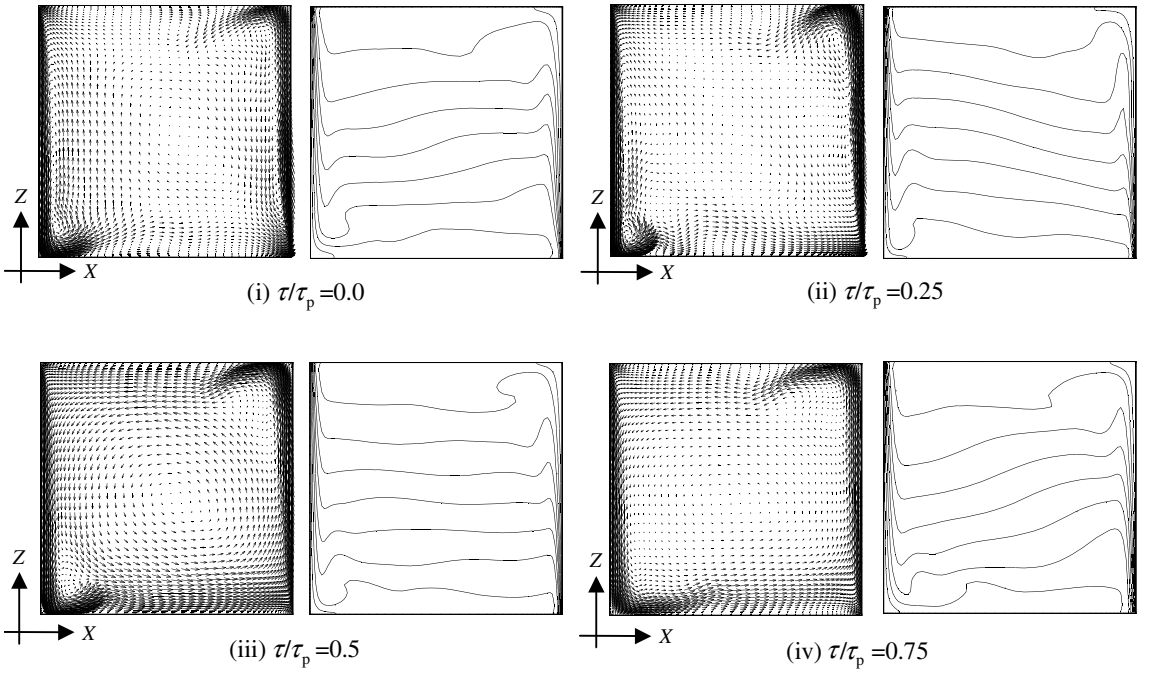

Fig. 7. Time histories of the thermal and velocity fields at $Y = 0.5$ plane under resonance ($Ra = 10^7$, $Pr = 0.7$, $\gamma = 10.0$, $\omega = 0.85$, $\Delta\theta = 0.1$).

4. Conclusions

Buoyant convection in a cubic enclosure under the combined effects of magnetizing and gravitational forces is studied. An electronic coil is placed below the bottom wall. Under the steady magnetic field in the zero-gravity environment, the thermal and temperature fields are akin to those of the conventional buoyant convection in a differentially-heated cavity in the constant-gravity environment.

For the cases of time-periodic magnetic field under constant gravity, the computed results suggest that resonance takes place when the frequency of external forcing matches the basic mode of internal gravity oscillations. At the resonance frequency, $A(Nu_{X=0.5})$ is maximized and convective activities in the interior are intensified. These resonance phenomena are similar to those of [6–12], which considered the resonance phenomena with the thermal or mechanical forcing.

The finding in the present work suggests that the resonant convection in a cube can be accomplished by a relatively simple way by applying a time-periodic magnetic forcing.

Acknowledgments

Appreciation is extended to the referees for constructive and helpful comments. This work was supported by the Grant [KRF-2003-041-D00129] from the Korea Research Foundation.

References

[1] B. Bai, A. Yabe, J. Qi, N.I. Wakayama, Quantitative analysis of air convection caused by magnetic-fluid coupling, AIAA J. 37 (1999) 1538–1543.
[2] N.I. Wakayama, H. Ito, Y. Kuroda, O. Fujita, K. Ito, Magnetic support of combustion in diffusion flames under microgravity, Combust. Flame 107 (1996) 187–192.
[3] T. Tagawa, R. Shigemitsu, H. Ozoe, Magnetizing force modeled and numerically solved for natural convection of air in a cubic enclosure: effect of the direction of the magnetic field, Int. J. Heat Mass Transfer 45 (2002) 267–277.
[4] R. Shigemitsu, T. Tagawa, H. Ozoe, Numerical computation for natural convection of air in a cubic enclosure under combination of magnetizing and gravitational forces, Numer. Heat Transfer, Part A 43 (2003) 449–463.
[5] T. Tagawa, A. Ujijhara, H. Ozoe, Numerical computation for Rayleigh–Benard convection of water in a magnetic field, Int. J. Heat Mass Transfer 46 (2003) 4097–4104.
[6] J.L. Lage, A. Bejan, The resonance of natural convection in an enclosure heated periodically from the side, Int. J. Heat Mass Transfer 36 (1993) 2027–2038.
[7] B.V. Antohe, J.L. Lage, A dynamic thermal insulator: inducing resonance within a fluid saturated porous medium enclosure heated periodically from the side, Int. J. Heat Mass Transfer 37 (1994) 771–782.
[8] B.V. Antohe, J.L. Lage, Amplitude effect on convection induced by time-periodic horizontal heating, Int. J. Heat Mass Transfer 39 (1996) 1121–1133.
[9] H.S. Kwak, J.M. Hyun, Natural convection in an enclosure having a vertical sidewall with time-varying temperature, J. Fluid Mech. 329 (1996) 65–88.
[10] H.S. Kwak, K. Kuwahara, J.M. Hyun, Prediction of the resonance frequency of natural convection in an enclosure with time-periodic heating imposed on one sidewall, Int. J. Heat Mass Transfer 41 (1998) 3157–3160.
[11] H.S. Kwak, K. Kuwahara, J.M. Hyun, Resonant enhancement of natural convection heat transfer in a square enclosure, Int. J. Heat Mass Transfer 41 (1998) 2837–2846.
[12] K.H. Kim, J.M. Hyun, H.S. Kwak, Buoyant convection in a side-heated cavity under gravity and oscillations, Int. J. Heat Mass Transfer 44 (2001) 857–861.
[13] S.V. Patankar, Numerical Heat Transfer and Fluid Flow, Hemisphere/McGraw-Hill, New York, 1980.
[14] T. Hayase, J.A.C. Humphrey, R. Greif, A consistently formulated QUICK scheme for fast and stable convergence using finite-volume iterative calculation procedures, J. Comput. Phys. 98 (1992) 108–118.
[15] G. de Vahl Davis, Natural convection of air in a square cavity: a bench mark numerical solution, Int. J. Numer. Methods Fluids 3 (1983) 249–264.
[16] J. Patterson, J. Imberger, Unsteady natural convection in a rectangular cavity, J. Fluid Mech. 100 (1980) 65–86.
[17] J.M. Hyun, Unsteady buoyant convection in an enclosure, Adv. Heat Transfer 34 (1994) 277–320.
[18] T. Fusegi, J.M. Hyun, K. Kuwahara, A numerical study of 3D natural convection in a cubic: effects of the horizontal thermal boundary conditions, Fluid Dynamics Res. 8 (1991) 221–230.
[19] S. Paolucci, D.R. Chenoweth, Transient to chaos in a differentially heated vertical cavity, J. Fluid Mech. 201 (1989) 379–410.